Electrogenerated Chemiluminescence. 76. Excited Singlet State Emission vs Excimer Emission in Ter(9,9-diarylfluorene)s

Jai-Pil Choi,[†] Ken-Tsung Wong,[‡] You-Ming Chen,[‡] Jen-Kan Yu,[‡] Pi-Tai Chou,[‡] and Allen J. Bard*[,†]

Department of Chemistry and Biochemistry, The University of Texas at Austin, Austin, Texas 78712, and Department of Chemistry, National Taiwan University, 106, Taipei, Taiwan

Received: July 22, 2003

The electrochemistry and electrogenerated chemiluminescence (ECL) of two ter(9,9-diarylfluorene)s, TDAFs, were investigated. The ECL from these new blue emitters produced by ion annihilation showed spectra with significant emission at longer wavelengths and was different from their fluorescence spectra. This was ascribed to the formation of excimers. Excimer emission was not observed in ECL during the reduction of the TDAFs with benzoyl peroxide (BPO) as a coreactant, where the ECL spectra were essentially the same as their fluorescence spectra, consistent with the requirement of ion annihilation for excimer production. Excimer emission is not seen in fluorescence, even at relatively high concentrations, because of the short lifetime of ^{1}TDAF*. The quantum yields, ϕ_{ECL}, for the ECL by ion annihilation were 0.05% for TDAF-1 and 0.01% for TDAF-2. ECL with BPO as a coreactant produced 8% (TDAF-1) or 3% (TDAF-2) of the ECL intensity of $Ru(bpy)_3^{2+}$ generated under the same conditions (0.5 mM TDAF or $Ru(bpy)_3^{2+}$/5 mM BPO).

Introduction

Fluorene-based macromolecules, such as terfluorenes,[1−3] oligomeric fluorenes,[3−5] and polyfluorenes,[6−9] are of interest in organic light-emitting devices (OLED) because of their efficient blue-light emitting characteristics and good chemical and thermal stabilities. Among these, the TDAFs show good optical and electrochemical properties,[1] such as high fluorescence quantum yields in solution (99%) as well as in thin films (∼90%) of interest in OLEDs. They also have good carrier transport properties and show high mobility of both electrons and holes in amorphous films.[10] These TDAFs are, therefore, good candidates for blue-light emitters in ECL.

ECL is light emission produced by an energetic electron transfer reaction between electrochemically generated species at an electrode. There are two general methods for producing ECL:

(1) An ion annihilation reaction that involves the generation of radical cations and radical anions on the electrode by alternating or sweeping potentials. The two oppositely charged species can undergo an electron transfer (ET) reaction (ion annihilation) in the diffusion layer of the electrode to produce the excited singlet or triplet state depending on the energy of the reaction. If the magnitude of the enthalpy (ΔH_{ann}) of an ion annihilation reaction is larger than the energy (E_s) needed for the excited singlet state, the direct generation of an excited singlet state is possible, as shown in Scheme 1; this is called the S-route or an energy-sufficient system.[11]

Scheme 1

$$R - e \rightarrow R^{\bullet +} \quad (1)$$

$$R + e \rightarrow R^{\bullet -} \quad (2)$$

$$R^{\bullet +} + R^{\bullet -} \rightarrow {}^1R^* + R \quad (3)$$

$${}^1R^* \rightarrow R + h\nu \quad (4)$$

where R is an emitter.

If $|\Delta H_{ann}|$ of the ion annihilation reaction is lower than E_s of the excited singlet state, but higher than the triplet state energy (E_t), the generation of an excited singlet state is still possible by triplet−triplet annihilation reaction as shown in Scheme 2 (a T-route or energy-deficient system).[11]

Scheme 2

$$R - e \rightarrow R^{\bullet +} \quad (1)$$

$$R + e \rightarrow R^{\bullet -} \quad (2)$$

$$R^{\bullet +} + R^{\bullet -} \rightarrow {}^3R^* + R \quad (5)$$

$${}^3R^* + {}^3R^* \rightarrow {}^1R^* + R \quad (6)$$

$${}^1R^* \rightarrow R + h\nu \quad (4)$$

where R is an emitter.

(2) Use of a coreactant (a compound that can produce a strong reducing or oxidizing agent by a reaction that follows the electrochemical ET reaction). These agents must be energetic enough to reduce or oxidize radical ions of emitters to their excited states. Typical coreactants for oxidations are tri-*n*-propylamine (TPrA), which produces a strong reducing agent (TPrA free radical, $TPrA^{\bullet}$)[12−15] and a relatively strong oxidizing agent (TPrA radical cation, $TPrA^{\bullet +}$)[16] and oxalate ion ($C_2O_4^{2-}$), which produces a strong reducing agent ($CO_2^{\bullet -}$).[17−19] Peroxy-

* To whom correspondence should be addressed. E-mail: ajbard@mail.utexas.edu.
† The University of Texas at Austin.
‡ National Taiwan University.

10.1021/jp036140n CCC: $25.00 © 2003 American Chemical Society
Published on Web 11/25/2003

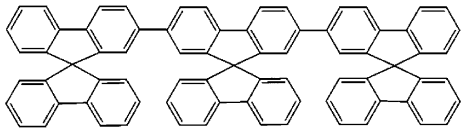

TDAF-1

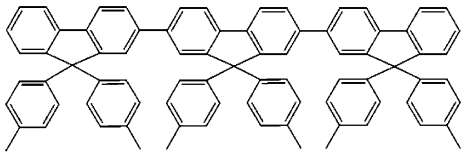

TDAF-2

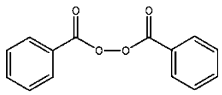

BPO

Figure 1. Molecular structure of TDAF-1, TDAF-2, and BPO.

disulfate ($S_2O_8^{2-}$) produces a strong oxidizing agent ($SO_4^{\bullet -}$)[20-22] upon reduction. The general ECL mechanism for a coreactant reduction is shown in Scheme 3.

Scheme 3

$$R + e \rightarrow R^{\bullet -} \quad (7)$$

$$CR + e \rightarrow CR^{\bullet -} \quad (8)$$

$$CR^{\bullet -} \rightarrow X \quad (9)$$

$$R^{\bullet -} + X \rightarrow {}^1R^* \text{ (or } {}^3R^*) + X' \quad (10)$$

where R is an emitter, CR is a coreactant, X is a reactive oxidizing agent produced from CR radical anion, and X′ is a reaction product of X.

For ion annihilation ECL, both the radical cations and radical anions should be relatively stable, but for coreactant ECL only one of the emitter radical ions needs to be stable. In this paper, we report the photophysical properties, electrochemistry, and ECL of two different ter(9,9-diarylfluorene)s, TDAF-1, and TDAF-2 shown in Figure 1. Moreover, ECL by both ion annihilation and coreactant ECL processes are described. We also demonstrate evidence for excimer emission of TDAF-1 and TDAF-2 by comparing the ECL spectra obtained by both approaches and, in addition, to their fluorescence spectra.

Experimental Section

Chemicals. The synthesis of TDAF-1 and TDAF-2 has been described.[1] Anhydrous acetonitrile (MeCN, 99.93% in a sure-sealed bottle), anhydrous benzene (Bz, 99.9% in a sure-sealed bottle), tetra-*n*-butylammonium perchlorate (TBAP), and BPO were obtained from Aldrich (St. Louis, MO) and used as received. TBAP and BPO were dried at 30 °C in a vacuum oven before transferring to an inert atmosphere drybox (Vacuum Atmospheres Co., Hawthorne, CA).

Apparatus and Instrumentation. UV−vis absorption and photoluminescence spectra were taken with a Milton Roy Spectronic 3000 array spectrophotometer and a Fluorolog-3 spectrofluorimeter (ISA-Jobin Yvon Hariba, Edison, NJ) using a 1 cm path-length quartz cuvette, respectively. The phosphorescence spectrum was measured by an ultrasensitive detection system coupled with a laser excitation source. Briefly, an Nd:YAG (355 nm, 8 ns, Continuum Surelite II) pumped optical parametric oscillator coupled with a second harmonic device serves as a tunable excitation source. The resulting emission was detected by an intensified charge-coupled device camera (ICCD, Princeton Instrument, Model 576G/1). The delay between pump laser and high voltage pulse amplifier (Princeton Instrument, PG 200) used to gate ICCD was controlled by a programmable delay pulse generator (SRS Model DG-535). The sample for the phosphorescence study was prepared in methylcyclohexane that forms a clear glass at 77 K and was degassed via three freeze−pump−thaw cycles prior to the measurement.

Cyclic voltammograms (CVs) were measured with a CH Instruments Electrochemical Work Station (Austin, TX) using a three-electrode conventional electrochemical cell. Platinum disk (area, 0.12 cm^2) and Pt wire served as the working and auxiliary electrodes, respectively. A silver (Ag) wire was used as a quasi-reference electrode (QRE) and all potentials were calibrated by adding ferrocene (Fc) as an internal reference and quoting all potentials vs SCE by taking Fc^+/Fc as 0.424 V vs SCE.[23]

All ECL measurements were performed as previously reported.[24] The ECL spectra were taken using a charge-coupled device (CCD) camera (Photometrics CH 260, Photometrics-Roper Scientific, Tucson, AZ). The CCD camera was aligned with the outlet of a grating spectrometer (concave grating, 1 mm entrance slit) calibrated with a mercury lamp emission. ECL spectra were obtained with 0.1 s potential pulses and at least 5 min of integration time.

Calculations. The optimized radical structures of TDAF-1 and TDAF-2 were obtained using the Spartan software package.

Results and Discussion

Absorbance, Fluorescence, and Phosphorescence. Absorption, fluorescence, and phosphorescence spectra of TDAF-1 and TDAF-2 are shown in Figure 2. The absorption and fluorescence spectra were obtained in the same solvent system, a 1:1 volume mixture of MeCN and Bz, which was also used for all electrochemical and ECL measurements. TDAF-1 and TDAF-2 gave absorption maxima at 351 and 353 nm, respectively, with the onset of these bands at around 398 nm (Figure 2a,b). Unlike TDAF-2, the absorption spectrum of TDAF-1 shows three additional absorption peaks at 263, 298, and 309 nm aside from the most intense absorption band at 351 nm. A comparison of the two absorbance spectra taken in 10 μM and 0.25 mM indicated that no aggregation of the ground states occurred at the higher concentration. There were no wavelength shifts found for TDAF-1 and TDAF-2 up to 0.25 mM (see Supporting Information). The fluorescence of the TDAFs, taken with excitation at the absorption maxima, displayed almost identical emission spectra with two well-resolved vibronic peaks and one shoulder (Figure 2a,b). No other luminescence above 500 nm was found. Phosphorescence spectra (Figure 2c) were obtained in a 77 K glassy methylcyclohexane medium with excitation at 355 nm. Phosphorescence maxima were observed at 525 nm for both TDAF-1 and TDAF-2, and the shape of the phosphorescence peak was very similar to that of the fluorescence. No phosphorescence could be observed at room temperature. All spectroscopic data are summarized in Table 1.

Electrochemistry. All electrochemical measurements were carried out in 1:1 volume mixture of MeCN and Bz with 0.1 M TBAP as supporting electrolyte with a Pt disk electrode. TDAF-1 and TDAF-2 show low solubility in pure MeCN. Although they have good solubility in CH_2Cl_2 and tetrahydro-

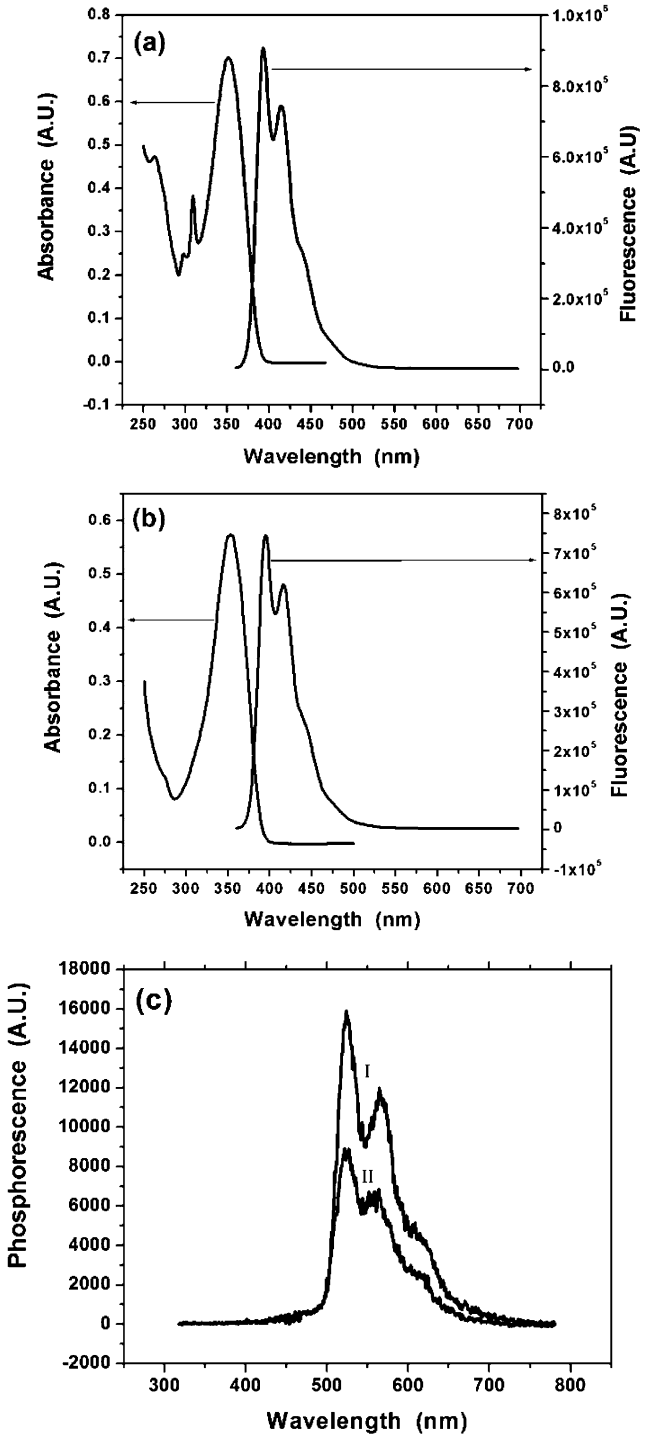

Figure 2. Absorption and fluorescence ($\lambda_{ex} = 350$ nm) spectra of (a) TDAF-1 and (b) TDAF-2 in MeCN:Bz (1:1, v:v) at room temperature under atmospheric conditions. Absorbance: 10 μM of TDAF. Fluorescence: 1 μM of TDAF. (c) Phosphorescence ($\lambda_{ex} = 355$ nm) spectra of 10.1 μM TDAF-1 (I) and 9.8 μM TDAF-2 (II) obtained at 77 K in deoxygenated methylcyclohexane. The spectra were taken at a delay time of 5 ms.

furan (THF),[1] these solvents are not appropriate for ECL because they have narrow potential windows. CVs of TDAF-1 and TDAF-2 are shown in Figure 3. When the potential was anodically swept at 0.1 V/s, two oxidation peaks were observed at 1.54 and 1.71 V (TDAF-1) and at 1.57 and 1.71 V (vs SCE) (TDAF-2). For a cathodic sweep, two reduction peaks were observed at −1.96 and −2.09 V (TDAF-1) and at −1.90 and −2.07 V (vs SCE) (TDAF-2). Although the cathodic reduction

TABLE 1: Summary of Spectroscopic Data[a]

	absorbance (nm)	fluorescence (nm)	phosphorescence (nm)
TDAF-1	263 (p), 298 (p), 309 (p), 351 (p)	393 (p), 414 (p), 440 (s)	525 (p), 570 (p), 620 (s)
TDAF-2	353 (p)	395 (p), 416 (p), 442 (s)	525 (p), 567 (p), 620 (s)

[a] p represents peak and s represents shoulder.

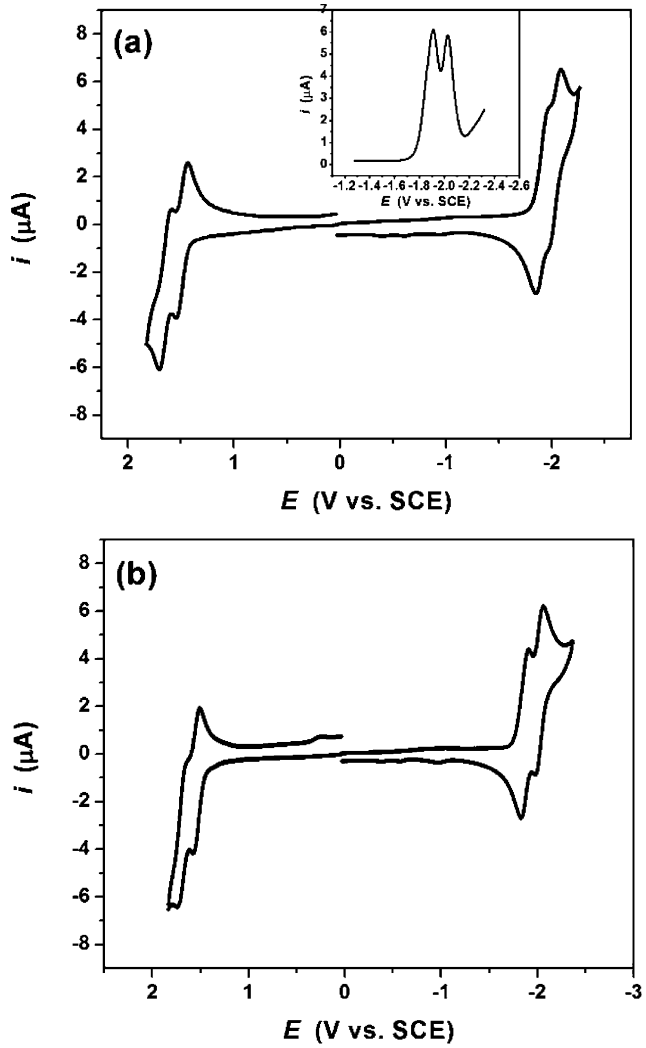

Figure 3. CVs of (a) 0.5 mM TDAF-1 and (b) 0.5 mM TDAF-2 in MeCN:Bz (1:1, v:v)/0.1 M TBAP at 0.1 V/s. Inset: DPV with increment potential 4 mV, amplitude 0.05 V, pulse width 0.05 s.

waves of TDAF-1 were not well-resolved, a differential pulse voltammogram, (DPV), (inset of Figure 3a) showed that TDAF-1 had two cathodic reductions such as TDAF-2. These electrochemical results are in good agreement with previous results in CH_2Cl_2 (oxidation) and THF (reduction).[1]

The oxidations and reductions of the TDAFs are essentially nernstian one-electron steps as judged from the peak potential separation (ΔE_p) compared to that of ferrocene (Fc) as an internal reference. Because of the ohmic drop caused by our solvent, ΔE_p is larger than the theoretical value of 59 mV. Under the same conditions, ΔE_p of Fc, which undergoes a nernstian reaction in this solvent, was 100 mV and this was about the same as the ΔE_p values of the TDAFs. The small potential separation between the first and the second reductions prevented a precise measurement of the current ratio even at slow scan

TABLE 2: Summary of Electrochemical Data

	oxidation		reduction	
	$E_{1/2}^{second}$ (V[a])	$E_{1/2}^{first}$ (V[a])	$E_{1/2}^{first}$ (V[a])	$E_{1/2}^{second}$ (V[a])
TDAF-1	+1.66	+1.49	−1.91	−2.02
TDAF-2	+1.70	+1.54	−1.87	−2.03

[a] V vs SCE. Scan rate = 0.1 V/s. In MeCN:Bz (1:1, v:v) containing 0.1 M TBAP.

rates (e.g., 20 mV/s). All half-wave potentials ($E_{1/2}$) of oxidations and reductions are summarized in Table 2.

Electrogenerated Chemiluminescence (ECL): Ion Annihilation. Because the electrochemical results show that the electrogenerated radical ions of both TDAFs are stable, ECL was initially performed by ion annihilation. The energy available in this ion annihilation reaction is given by[11]

$$|\Delta H_{ann}| \cong E_p(\text{TDAF/TDAF}^{\bullet+}) - E_p(\text{TDAF/TDAF}^{\bullet-}) - 0.1 \quad (11)$$

For S-route ion annihilation, $|\Delta H_{ann}|$ must be larger than the lowest excited singlet energy (E_s), as calculated from the fluorescence emission peak; data for the TDAFs, summarized in Table 3, suggest that ECL via the S-route is possible.

ECL was obtained by continuously pulsing (pulse width = 0.1 s) the potential of a Pt working electrode between +1.58 and −1.95 V vs Ag QRE for TDAF-1 or +1.54 and −1.97 V vs Ag QRE for TDAF-2. The ECL of the TDAFs (Figure 4), unlike their fluorescence (which showed no emission beyond 500 nm), produced the most intense emissions at much longer wavelengths. The emission bands were quite broad and centered at 522 nm for TDAF-1 and 583 nm for TDAF-2. The bandwidth at a half emission intensity was about 300 nm. Less intense ECL emissions corresponding to the fluorescence, at 406 nm for TDAF-1 and 410 nm for TDAF-2 were also present. The lack of resolution in the ECL spectra at the shorter wavelengths compared to the fluorescence can be ascribed to the wide entrance slit (1 mm) of a grating spectrometer used for ECL because of the low ECL intensity. Thus, the shorter wavelength ECL with a shoulder at ~400 nm can be ascribed to emission from the lowest singlet state (Figure 5 path a).

The unusually broad ECL emission of the TDAFs could come from byproducts from side reactions of the radical ions, excimers, or triplet states. Immediately after the ECL experiments, the solution fluorescence spectra were measured again and found to be identical to those measured before ECL experiments, suggesting there were no side reactions to produce bulk byproducts fluorescing at longer wavelengths (although small amounts produced in the diffusion layer near the electrode that emit is still a possibility) (see Supporting Information).

The second possibility is the formation of an excimer. Generally, excimers generate structureless broad emission bands. Although the ECL spectra of the TDAFs were quite broad (~300 nm bandwidth), they were not structureless and appear to have shoulders at around 750 nm in addition to the broad bands (Figure 4). These shoulders, however, are artifacts caused by the second harmonic signals of the lowest excited singlet state emissions. If a long-wavelength pass (LP) filter of 425 nm was placed in front of the CCD camera and ECL by ion annihilation was measured, the spectra did not show these shoulders (see Supporting Information). The formation of excimer is more favorable in this ECL than in photoluminescence, because ion annihilation involves the collision of oppositely charged radical ions. The proposed mechanism for excimer formation in ECL is shown in Figure 5 path b. Most excimers were formed through the path b route rather than by reaction of excited state and ground state (Figure 5 path c), because no excimer emission was found in the fluorescence spectra. Lack of excimer formation in fluorescence can be ascribed to the relatively short radiative lifetimes (840 ps, TDAF-1 and 790 ps, TDAF-2) compared with average fluorescence lifetime[25] of 10^{-9} to 10^{-8} s for a singlet excited state. Thus, the rate of decay of ^{1}(TDAF)* was probably so fast that excimer formation by path (c) would be negligible in both fluorescence and ECL. In addition, the bulky substituent groups (biphenyl for TDAF-1 and *p*-toluenyl for TDAF-2) would make path (c) much slower due to the steric hindrance. Similar results were reported for a polyfluorene.[26]

Electrogenerated Chemiluminescence (ECL): Coreactant. To test for the importance of annihilation in the production of excimer, an ECL experiment was performed using the coreactant, BPO. When BPO is electrochemically reduced at −1.23 V vs SCE, the reaction proceeds through the ECE route[27] to produce the benzoate radical ($C_6H_5CO_2^{\bullet}$) that is a strong oxidizing agent (Scheme 4). This follows an early study by Chandross and Sonntag[28] where BPO was reduced stepwise by hydrocarbon radical anions rather than at an electrode.

Scheme 4

$$\text{BPO} + e \rightarrow \text{BPO}^{\bullet-} \quad (12)$$

$$\text{BPO}^{\bullet-} \rightarrow C_6H_5CO_2^- + C_6H_5CO_2^{\bullet} \quad (13)$$

$$C_6H_5CO_2^{\bullet} + e \rightarrow C_6H_5CO_2^- \quad (14)$$

Figure 6 shows the ECL spectra (solid line) of the TDAFs in MeCN:Bz (1:1, v:v)/0.1 M TBAP at a Pt electrode with 0.1 s potential pulses from 0 to −1.96 V vs Ag QRE for TDAF-1 or 0 to −1.98 V vs Ag QRE for TDAF-2. Under these conditions only radical anions of TDAF-1 and TDAF-2 and $C_6H_5CO_2^{\bullet}$ were produced. Unlike the ECL spectra by ion annihilation, these ECL spectra displayed only emission corresponding to the fluorescence emission (dotted line in Figure 6) with no evidence of excimer emission.

The energy available in the reaction between the radical anions and $C_6H_5CO_2^{\bullet}$ can be calculated by eq 11, using $E°(C_6H_5CO_2^{\bullet}/C_6H_5CO_2^-)$. Two different $E°$ values for a $C_6H_5CO_2^{\bullet}/C_6H_5CO_2^-$ couple have been reported: +1.5 V vs SCE[28] and +0.8 V vs SCE.[29] If we use the larger value, the energy of reaction 16 was 3.36 eV for TDAF-1 and 3.30 eV for TDAF-2, in both cases sufficient to form the lowest excited singlet state (3.16 eV) directly and the suggested mechanism is in Scheme 5.

Scheme 5

$$\text{BPO} + e \rightarrow \text{BPO}^{\bullet-} \quad (12)$$

$$\text{BPO}^{\bullet-} \rightarrow C_6H_5CO_2^- + C_6H_5CO_2^{\bullet} \quad (13)$$

$$\text{TDAF} + e \rightarrow \text{TDAF}^{\bullet-} \quad (15)$$

$$\text{TDAF}^{\bullet-} + C_6H_5CO_2^{\bullet} \rightarrow {}^1\text{TDAF}^* + C_6H_5CO_2^- \quad (16)$$

$${}^1\text{TDAF}^* \rightarrow \text{TDAF} + h\nu \quad (17)$$

If +0.8 V vs SCE is used as $E°(C_6H_5CO_2^{\bullet}/C_6H_5CO_2^-)$,[29] the energy is 2.66 eV for TDAF-1 and 2.60 eV for TDAF-2. These energies are below that of the lowest singlet excited state (3.16

TABLE 3: Physical Data of Ion Annihilation Reaction and Coreactant Reaction for ECL

	$E_{p,a}$ (V)[a]	$E_{p,c}$ (V)[b]	$-\Delta G$ (eV)[c]	$-\Delta H$ (eV)[d]	E_s (eV)[e]	E_t (eV)[e]	ΔE^* (eV)[f]
TDAF-1	+1.54	−1.96	3.50	3.40	3.16	2.38	
TDAF-1 + BPO	+1.5[g]	−1.96	3.46	3.36	3.16	2.38	−0.29
	+0.8[h]	−1.96	2.76	2.66	3.16	2.38	
TDAF-2	+1.57	−1.90	3.47	3.37	3.16	2.38	
TDAF-2 + BPO	+1.5[g]	−1.90	3.40	3.30	3.16	2.38	−0.32
	+0.8[h]	−1.90	2.70	2.60	3.16	2.38	

[a] Anodic peak potential, V vs SCE. In MeCN:Bz (1:1, v,v) containing 0.1 M TBAP. [b] Cathodic peak potential of TDAFs, V vs SCE. [c] $-\Delta G = E_{p,a} - E_{p,c}$. [d] $-\Delta H_{ann}$ or $-\Delta H_{co}$. $-\Delta H = -\Delta G - 0.1$. [e] Calculated from the spectroscopic data. [f] $\Delta E^* = E_t + E_p(\text{BPO/BPO}^-) - E_p(\text{TDAF/TDAF}^{\bullet+}) + 0.1$. [g] $E°$ of $C_6H_5CO_2^\bullet$ from ref 28. [h] $E°$ of $C_6H_5CO_2^\bullet$ from ref 30.

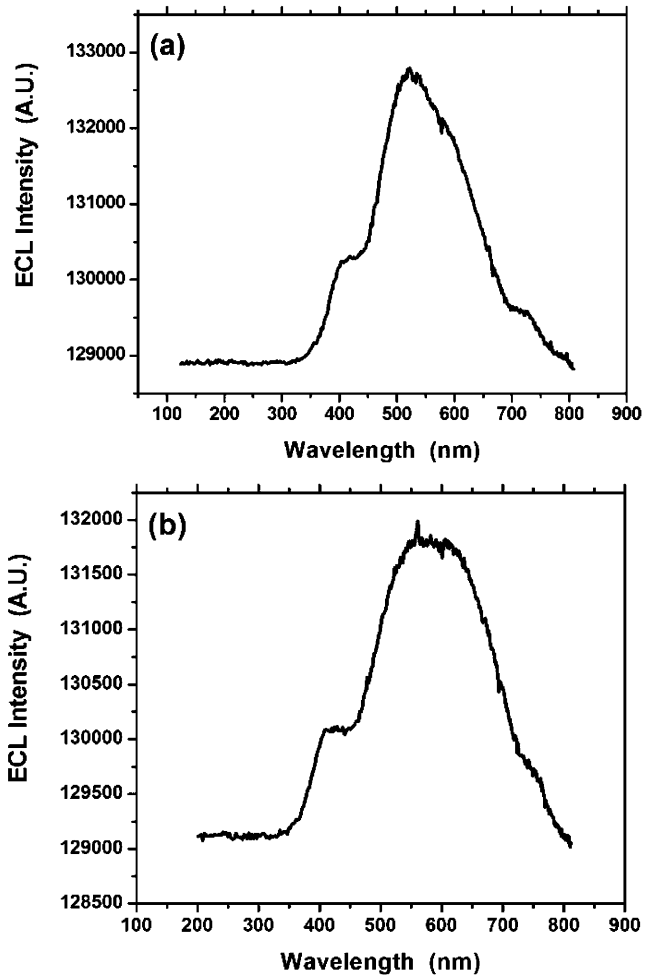

Figure 4. ECL spectra of (a) 0.5 mM TDAF-1 and (b) 0.5 mM TDAF-2 in MeCN:Bz (1:1, v:v)/0.1 M TBAP. 0.1 s pulses by alternating between +1.58 and −1.95 V vs Ag QRE for (a) and +1.54 and −1.97 V vs Ag QRE for (b). All spectra were obtained with an integration time of 5 min.

eV); so one cannot produce ^{1}TDAF* directly. However, both 2.66 and 2.60 eV are large enough to produce ^{3}TDAF* (2.38 eV) with ^{1}TDAF* generated by triplet−triplet annihilation:

$$\text{TDAF}^{\bullet-} + \text{C}_6\text{H}_5\text{CO}_2^\bullet \rightarrow {}^3\text{TDAF}^* + \text{C}_6\text{H}_5\text{CO}_2^- \quad (18)$$

$$^3\text{TDAF}^* + {}^3\text{TDAF}^* \rightarrow {}^1\text{TDAF}^* + \text{TADF} \quad (19)$$

Once the triplet state is formed, it is possible to produce $\text{TDAF}^{\bullet+}$ by triplet state quenching, eq 20, which could then lead to some excimer formation. To determine the energy change (ΔE^*) for eq 20, the triplet state energy, E_t, of TDAF and the free energy of eq 21 were used.

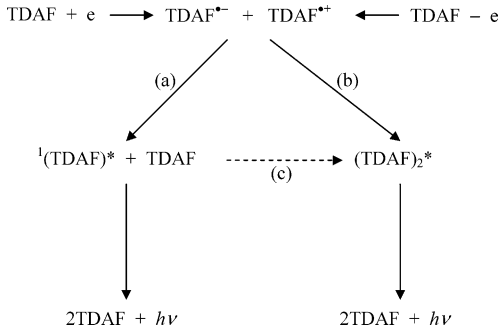

Figure 5. Schematic diagram of ECL and excimer formation mechanism.

$$^3\text{TDAF}^* + \text{BPO} \rightarrow \text{TDAF}^{\bullet+} + \text{BPO}^- \quad (20)$$

$$\text{TDAF} + \text{BPO} \rightarrow \text{TDAF}^{\bullet+} + \text{BPO}^- \quad (21)$$

$$\Delta E^* = E_t + E_p(\text{BPO/BPO}^-) - E_p(\text{TDAF/TDAF}^{\bullet+}) + 0.1 \quad (22)$$

The $E°$ of the BPO/BPO$^-$ couple is needed to calculate the enthalpy for reaction 21, but the electrochemical reduction of BPO occurs via ECE reaction and is irreversible as described previously. The irreversible peak potential (−1.23 V vs SCE) of BPO/BPO$^-$ is less negative than $E°_{\text{BPO/BPO}-}$, so it would represent a lower limit for the energy of (21).[30] ΔE^* values calculated in this way are summarized in Table 3; these suggest that reaction 20 is nonspontaneous. However, this estimate is compromised by the use of the experimental irreversible E_p value. The radical $C_6H_5CO_2^\bullet$ could oxidize TDAF to $\text{TDAF}^{\bullet+}$ and lead to the formation of excimers, but this reaction is energetically marginal, because for $C_6H_5CO_2^\bullet/C_6H_5CO_2^-$, $E° = +1.5$ V (maximum) and for $\text{TDAF}^{\bullet+}$/TDAF, $E° = +1.54$ V (at least). Therefore, the absence of $\text{TDAF}^{\bullet+}$ and excimers in ECL by BPO is understandable.

Modeling the Excimer. The presence of bulky substituent groups in a molecule can prevent formation of excimers[31] and high dielectric constant solvents, such as MeCN and DMSO, typically show less excimer emission than low dielectric solvents such as THF.[32] However, formation of excimers in ECL by ion annihilation can be a very efficient process because the excited state is formed by two reactants in close proximity, just as with exciplexes studied by ECL.[32] The rate of exciplex formation is governed by the overlap of π orbitals in the molecules and Coulombic interactions between oppositely charged species.[33] Therefore, formation of TDAF excimers can be very efficient in ion annihilation, even if the TDAFs have bulky substituents and a high dielectric solvent is used.

To model the proposed excimer, geometric optimization calculations were performed for $[\text{TDAF-1}]^{\bullet+}$ and $[\text{TDAF-1}]^{\bullet-}$ using molecular dynamics and then an excimer model was

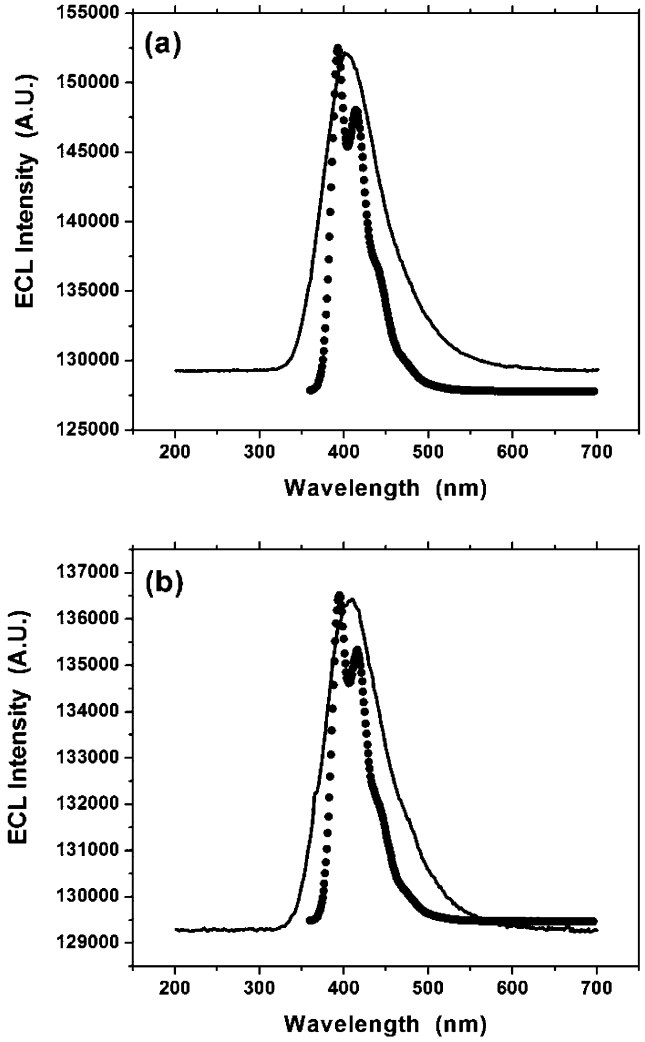

Figure 6. ECL (solid line) spectra of (a) 0.5 mM TDAF-1 and (b) 0.5 mM TDAF-2 with 5 mM BPO in MeCN:Bz (1:1, v:v)/ 0.1 M TBAP. 0.1 s pulses alternating 0 and −1.96 V vs Ag QRE for (a) and 0 and −1.98 V vs Ag QRE for (b). All ECL spectra were obtained with an integration time of 5 min. Fluorescence spectra (dotted line) were obtained with (a) 1 μM TDAF-1 and (b) 1 μM TDAF-2 without BPO. $\lambda_{ex} = 350$ nm for both (a) and (b).

manually constructed by manipulating the orientation of the two radical ions and placing them in close proximity. Figure 7 shows a possible ionic dimer before the excimer is produced by ion annihilation. Here, the fluorene backbones totally overlap to allow a $\pi-\pi$ orbital stacking as well of the biphenyl groups, and this dimer can be stabilized by Coulombic interaction between $[TDAF\text{-}1]^{\bullet+}$ and $[TDAF\text{-}1]^{\bullet-}$. Although there is some steric hindrance between the biphenyl groups, some rearrangement could occur to minimize it.

Triplet ECL Emission. It is unlikely that the long wavelength ECL emission is triplet state emission, which is generally very weak at room temperature because of its long radiative lifetime (>1.0 s) and quenching by molecular oxygen and other species. Rothe and Monkman[34] investigated the temperature dependence of phosphorescence of poly(9,9-bis(ethylhexyl)fluorene), which was similar to TDAF, and did not observe phosphorescence above 80 K. No phosphorescent emission of the TDAFs was found above 77 K in our experiments. Moreover, if the long wavelength ECL emission were from the triplet state, it should appear in the ECL spectra with a coreactant as well as by ion annihilation.

ECL Efficiency. The relative ECL efficiency (ϕ_{ECL}) was calculated from eq 23[35] using a ϕ°_{ECL} (~5%)[36] for $Ru(bpy)_3^{2+}$ as a reference

$$\phi_{ECL} = (\phi^\circ_{ECL} \cdot I_{ECL} \cdot Q^\circ_{a,c})/(I^\circ_{ECL} \cdot Q_{a,c}) \qquad (23)$$

where I_{ECL} is the integrated ECL intensity and $Q_{a,c}$ is the total anodic or cathodic charge. The estimated ϕ_{ECL} was 0.05% for TDAF-1 and 0.01% for TDAF-2 by ion annihilation ECL. However, it was not possible to calculate ϕ_{ECL} in coreactant ECL, because the total charge did not represent the number of reactions between $TDAF^{\bullet-}$ and $C_6H_5CO_2^\bullet$. Therefore, ECL of $Ru(bpy)_3^{2+}$ with BPO was employed as a reference, although this ECL system has not been previously reported. The generation of $Ru(bpy)_3^{2+*}$ can be described by a similar mechanism as that in Scheme 5; the electrochemically generated $Ru(bpy)_3^{+}$ reacts with $C_6H_5CO_2^\bullet$ to produce $Ru(bpy)_3^{2+*}$. Because $C_6H_5CO_2^\bullet$ ($E^\circ = +1.5$ V vs SCE) is sufficiently energetic, $Ru(bpy)_3^{2+}$ could also be oxidized to $Ru(bpy)_3^{3+}$ (E° of $Ru(bpy)_3^{2+/3+} = +1.25$ V vs SCE).[37] As a result, $Ru(bpy)_3^{2+*}$ could also be produced by the annihilation reaction of $Ru(bpy)_3^{3+}$ and $Ru(bpy)_3^{+}$. The integrated ECL intensity ratio of TDAF to $Ru(bpy)_3^{2+}$ under exactly the same experimental conditions (0.5 mM TDAF or $Ru(bpy)_3^{2+}$/5 mM BPO) was expressed instead of ϕ_{ECL}. The estimated percentage of I(TDAF)/$I(Ru(bpy)_3^{2+})$ was 8% for TDAF-1 and 3% for TDAF-2. Because of the lack of excimer formation, ECL produced with BPO yielded a stronger and purer blue emission than ECL by ion annihilation.

Conclusions

TDAF-1 and TDAF-2 are new blue ECL emitters. For both compounds, ECL by ion annihilation produced excimer emis-

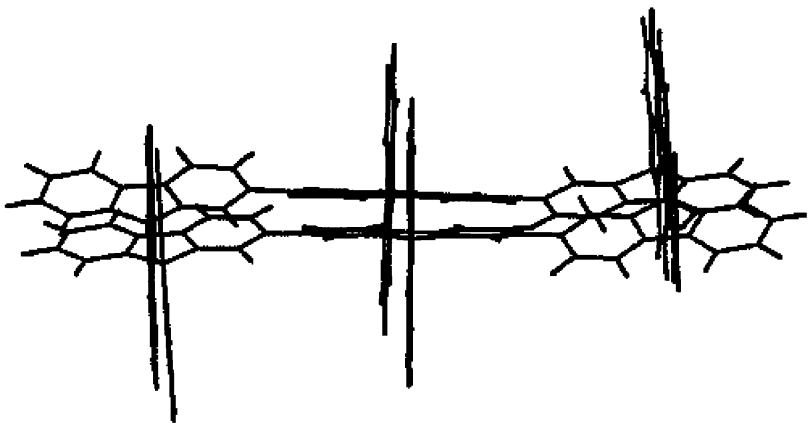

Figure 7. Model of a dimer of TDAF-1 from radical ions.

sion, which was not seen in the fluorescence spectra. In this process, the formation of excimers was mainly from a reaction of oppositely charged radical ions (Figure 5, path b). ECL produced by reduction in the presence of BPO coreactant only produced emission at the fluorescence (monomer) wavelengths, supporting the formation of excimer only by ion annihilation.

Acknowledgment. We thank Dr. Don O'Connor, Center for Nano- and Molecular Science and Technology, The University of Texas at Austin, for helpful discussion of fluorescence lifetime measurements, and Mr. Hyunseok Hwang for operating the software for geometric optimization calculations. Funding by IGEN, Inc. and NSF (NSF grant CHE0109587) is gratefully acknowledged. K.T.W. thanks the National Science Council for the financial support (NSC-91-2113-M-002-025).

Supporting Information Available: UV−vis spectra of TDAF at low and high concentrations, fluorescence spectra measured after ECL experiments, and filtered and unfiltered ECL spectra are available. This material is available free of charge via the Internet at http://pubs.acs.org.

References and Notes

(1) Wong, K.-T.; Chien, Y.-Y.; Chen, R.-T.; Wang, C.-F.; Lin, Y.-T.; Chiang, H.-H.; Hsieh, P.-Y.; Wu, C.-C.; Chou, C. H.; Su, Y. O.; Lee, G.-H.; Peng, S.-M *J. Am. Chem. Soc.* **2002**, *124*, 11576.

(2) Geng, Y.; Katsis, D.; Culligan, S. W.; Ou, J. J.; Chen, S. H.; Rothberg, L. J. *Chem. Mater.* **2002**, *14*, 463.

(3) Katsis, D.; Geng, Y. H.; Ou, J. J.; Culligan, S. W.; Trajkovska, A.; Chen, S. H.; Rothberg, L. J. *Chem. Mater.* **2002**, *14*, 1332.

(4) Belletête, M.; Morin, J.-F.; Beaupré, S.; Ranger, M.; Leclerc, M.; Durocher, G. *Macromolecules* **2001**, *34*, 2288.

(5) Destri, S.; Pasini, M.; Botta, C.; Porzio, W.; Bertini, F.; Marchiò, L. *J. Mater. Chem.* **2002**, *12*, 924.

(6) Chang, S.-C.; Yang, Y.; Pei, Q. *Appl. Phys. Lett.* **1999**, *74*, 2081.

(7) Teetsov, J.; Fox, M. A. *J. Mater. Chem.* **1999**, *9*, 2117.

(8) Chang, S.-C.; Li, Y.; Yang, Y. *J. Phys. Chem.* **2000**, *104*, 11650.

(9) Lupton, J. M.; Craig, M. R.; Meijer, E. W. *Appl. Phys. Lett.* **2002**, *80*, 4489.

(10) Wu, C.-C.; Liu, T.-L.; Hung, W.-Y.; Lin, Y.-T.; Wong, K.-T.; Chen, R. −T, Chen, Y.-M.; Chien, Y.-Y. *J. Am. Chem. Soc.* **2003**, *125*, 3710.

(11) Faulkner, L. R.; Bard, A. J. In *Electroanalytical Chemistry*; Bard, A. J., Ed; Marcel Dekker: New York, 1977; Vol. 10, pp 1−95.

(12) Noffsinger, J. B.; Danielson, N. D. *Anal. Chem.* **1987**, *59*, 865.

(13) Leland, J. K.; Powell, M. J. *J. Electrochem. Soc.* **1990**, *137*, 3127.

(14) Zu, Y.; Bard, A. J. *Anal. Chem.* **2000**, *72*, 3223.

(15) Kanoufi, F.; Zu, Y.; Bard, A. J. *J. Phys. Chem. B* **2001**, *105*, 210.

(16) Miao, W.; Choi, J.-P.; Bard, A. J. *J. Am. Chem. Soc.* **2002**, *124*, 14478.

(17) Chang, M.-M.; Saji, T.; Bard, A. J. *J. Am. Chem. Soc.* **1977**, *99*, 5399.

(18) Rubinstein, I.; Bard, A. J. *J. Am. Chem. Soc.* **1981**, *103*, 512.

(19) Kanoufi, F.; Bard, A. J. *J. Phys. Chem. B* **1999**, *103*, 10469.

(20) White, H. S.; Bard, A. J. *J. Am. Chem. Soc.* **1982**, *104*, 6891.

(21) Becker, W. G.; Seung, H. S.; Bard, A. J. *J. Electroanal. Chem.* **1984**, *167*, 127.

(22) Fabrizio, E. F.; Prieto, I.; Bard, A. J. *J. Am. Chem. Soc.* **2000**, *122*, 4996.

(23) Debad, J. D.; Morris, J. C.; Magnus, P.; Bard, A. J. *J. Org. Chem.* **1997**, *62*, 530.

(24) McCord, P.; Bard, A. J. *J. Electroanal. Chem.* **1991**, *318*, 91.

(25) Parker, C. A. In *Photoluminescence of Solutions*; Elsevier Publishing Co.: New York, 1968; Chapter 1, p 38.

(26) Prieto, I.; Teetsov, J.; Fox, M. A.; Vanden Bout, D. A.; Bard, A. J. *J. Phys. Chem. A* **2001**, *105*, 520.

(27) Bard, A. J.; Faulkner, L. R. In *Electrochemical Methods*, 2nd ed.; John Wiley & Sons: New York, 2001; Chapter 12, p 476.

(28) Chandross, E. A.; Sonntag, F. I. *J. Am. Chem. Soc.* **1966**, *88*, 1089.

(29) Akins, D. L.; Birke, R. L. *Chem. Phys. Lett.* **1974**, *29*, 428.

(30) Santa Cruz, T. D.; Akins, D. L.; Birke, R. L. *J. Am. Chem. Soc.* **1976**, *98*, 1677.

(31) Birks, J. B. In *Photophysics of Aromatic Molecules*; Wiley-Interscience: New York, 1970; Chapter 7.

(32) Bard, A. J.; Park, S. M. In *The Exciplex*; Gordon, M.; Ware, W. R., Eds.; Academic Press: New York, 1975; p 305.

(33) Zachariasse, K. In *The Exciplex*; Gordon, M.; Ware, W. R., Eds.; Academic Press: New York, 1975; p 275.

(34) Rothe, C.; Monkman, A. *Phys. Rev. B* **2002**, *65*, 073201.

(35) Wallace, W. L.; Bard, A. J. *J. Phys. Chem.* **1979**, *83*, 1350.

(36) Tokel-Takvoryan, N. E.; Hemingway, R. E.; Bard, A. J. *J. Am. Chem. Soc.* **1973**, *95*, 6582.

(37) Taken from $E_{1/2}$ of $Ru(bpy)_3^{2+/3+}$ measured in MeCN:Bz (1:1, v:v)/0.1 M TBAP.